Antibacterial Efficacy Comparison of Electrolytic and Reductive Silver Nanoparticles Against Propionibacterium Acnes

Suparno Suparno *, Rita Prasetyowati , Khafidh Nur Aziz , Anggarwati Rahma , Eka Sentia Ayu Lestari , Siti Nabiila , Deby Grace

Posted Date: 12 December 2024

doi: 10.20944/preprints202412.0951.v1

Keywords: reduction; toxic free electrolysis; antibiotics; bacterial resistance; Kirby-Bauer method

Article

Antibacterial Efficacy Comparison of Electrolytic and Reductive Silver Nanoparticles Against Propionibacterium Acnes

Suparno Suparno [1,*], Rita Prasetyowati [1], Khafidh Nur Aziz [1], Anggarwati Rahma [1], Eka Sentia Ayu Lestari [1], Siti Nabiila [1] and Deby Grace [1]

Universitas Negeri Yogyakarta, 1st Colombo St., Karangmalang, Depok, Yogyakarta 55281, Indonesia
* Correspondence: suparno_mipa@uny.ac.id; Tel.: +6281 2271 9098, Fax: +62 274 548 203

Abstract: The increasing interest in developing silver nanoparticles as antibiotic raw materials has attracted much attention, as the most common reduction and electrolysis techniques produce the toxic gas byproduct nitrogen dioxide. This paper reports a successful effort to develop a modified toxic-free electrolysis technique to produce electrolytic silver nanoparticles (ESN). A comparison of the physical and biological properties of ESN and reductive silver nanoparticles (RSN) was made. The presence of silver atoms in the solution was determined using a UV visible spectrometer and absorption peaks were found at 425 nm (ESN) and 437 nm (RSN). The particle size in solution was determined using dynamic light scattering and the diameter was found to be approximately 40 nm (for ESN) and 70 nm (for RSN). Antibacterial efficacy and power to prevent the development of bacterial resistance against *Propionibacterium acnes* (*P. acnes*) were assessed using the Kirby-Bauer method. Statistical analysis of clear zone diameter data showed that unlike RSN, the efficacy of ESN increased with higher concentrations. The efficacy of ESN and RSN is relatively lower than Chloramphenicol 5% because it is measured in different concentration units (ESN and RSN in ppm and Chloramphenicol in %). By using a calibration curve, the efficacy of 5% Chloramphenicol can be equated to 0.005% ESN. In addition, P. acnes developed strong resistance to Chloramphenicol, weak resistance to RSN and showed no resistance to ESN. These findings underscore the extraordinary potential of ESN as a raw material for future antibiotics.

Keywords: reduction; toxic free electrolysis; antibiotics; bacterial resistance; Kirby-Bauer method

1. Introduction

Most bacteria develop drug resistance due to drug abuse, drug overuse, and long-term exposure to the same drug[1,2] . Using the wrong type of antibiotic will not cure the disease. It can even cause resistance to antibiotics. Overuse of drugs can kill some bacteria, but can develop resistance. Prolonged use of drugs may cause bacteria to develop resistance [3]. The development of bacterial resistance to many antibacterial agents is rapid [4,5]. Meanwhile, the discovery of new and more effective drugs is very slow [6].

Propionibacterium acnes (*P. acnes*) is a Gram-positive bacterium commonly found in the skin, oral cavity, and gastrointestinal tract [7]. This bacterium is aerobic, aerotolerant, commensal, and under certain condition it turns to become pathogenic [8]. *P. acnes* and *Staphylococcus aureus* are the major cause of pathogenic in acne. *P. acnes* was chosen for this research due to its susceptibility to many antibiotics, such as beta-lactams, quinolones, and rifampin and its continuing resistance development to new antibiotics [8]. These bacteria are known to develop biofilm [9] as part of their survival mechanisms [9,10].

Research in the development of antibiotic raw materials has been ongoing for decades. Medicinal plant-based raw materials have attracted much attention [11,12]. However, much research has been done to develop metal nanoparticles over the past 2-3 decades [13,14]. Plant-based antibiotics are relatively easy to prepare but take a long time to reproduce and it is difficult to maintain the sustainability of the raw materials. On the other hand, metal nanoparticles are relatively

 doi:10.20944/preprints202412.0951.v1

difficult to prepare, easy to reproduce, and the raw materials are abundant. The most widely studied metal nanoparticles as antibacterial agents today are silver nanoparticles for two reasons, namely relatively low cost, high efficacy [15].

The relatively high efficacy of silver nanoparticles is most likely due to their bactericidal properties. Silver nanoparticles not only inhibit bacterial growth but also kill them. Although the exact mechanism is still unknown, there are eight mechanisms proposed for silver nanoparticles to inhibit and kill bacteria as depicted in Figure 1. Figure 1 shows that there are two types of silver nanoparticle soldiers involved in fighting against bacteria namely "regular soldier" (a) silver nanoparticle and "special force" (b) silver ions. They combat bacteria in eight different ways simultaneously. (1) The accumulation of silver nanoparticles on the bacterial membrane causes cytoplasmic membrane denaturation causes organelles rupture and leads to the cell lysis [16]. (2) The very small size of silver nanoparticles allows them to penetrate the cell wall and change the membrane structure thereby inhibiting bacterial growth [17]. (3) Silver nanoparticles inhibit *P. acnes* biofilm production[18,19]. This may be due to the thermally conductive nature of the metal nanoparticles, which absorb heat and leave liquid biofilm dried. (4) Silver nanoparticles release silver ions and these ions bind to sulfur in bacterial cell wall proteins [18,20]. The adhesion of silver ions to the cell wall causes increased permeability and disrupts electrolyte flow, leading to membrane rupture and bacterial death [9]. (5) Silver ions interfere with the production of adenosine triphosphate, which results in a low energy source for bacteria [21]. This inhibits bacterial growth and can lead to bacterial death. (6) Silver ions cause denaturation of ribosomes in the cytoplasm, which disrupts protein synthesis and inhibits bacterial growth. (7) Silver ions in bacterial cells can inactivate respiratory enzymes, causing bacteria to suffocate and eventually die [22]. (8) Silver ions penetrate to bacterial cells and create reactive oxygen [23]. Reactive oxygen species induction causes modifications to DNA, disrupts DNA replication, and inhibits bacterial growth [24].

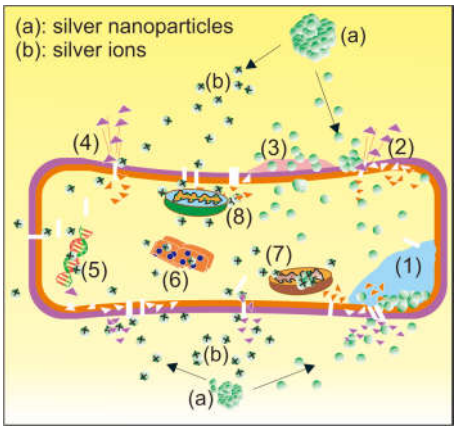

Figure 1. Possible mechanism of silver nanoparticles in killing and inhibiting bacteria.

There are two main techniques for producing silver nanoparticles, namely reduction and electrolysis techniques [25,26]. The reduction technique is carried out by mixing silver nitrate solution and trisodium citrate solution. Both solutions are mixed and heated in water using a magnetic stirrer. The reduction technique can produce reductive silver nanoparticles (RSN) quickly [27]. However, there are two problems that most people are not aware of. First, it produces citric acid and sodium hydroxide byproducts [28]. Citric acid contains three carboxyl functional groups per molecule known as a red-shifted auxochrome. This auxochrome absorbs some of the translational energy so that the peak absorption wavelength shifts to the red, to a lower energy. Second, it produces toxic byproduct [29,30]. Nitrogen dioxide (NO2) hazardous gas produced from the decomposition of HNO3 when silver nitrate was used as precursor. On the other hand, the electrolysis technique using silver nitrate as the electrolyte produces a silver solution that is free from contaminants (such as citric acid), but still produces the same toxic gas, NO2. *This inspired us to create a modified electrolysis technique to produce silver nanoparticles that are free from contaminants and toxic gases and observe their antibacterial properties*.

 doi:10.20944/preprints202412.0951.v1

The formation of silver nanoparticles in electrolytic and reductive techniques is highly dependent on the aggregation of silver atoms in solution [31]. The higher the concentration of silver atoms, the larger the size of silver nanoparticles. It is estimated that each silver nanoparticle contains 20 to 15000 silver atoms [32]. The short-range van der Waals attraction is the most likely cause of aggregation when atoms collide with each other due to Brownian motion [33]. Therefore, we believe that the physical characteristics of electrolytic silver nanoparticles (ESN) and RSN should be the same unless the environment around the silver nanoparticles changes them.

For now, we are more interested in exploring the biological characteristics of ESN and RSN especially on their antibiotic properties. Therefore, the observation of the antibacterial activity of ESN and RSN was carried out and compared with Chloramphenicol as a positive control. The focus of the observation was on the efficacy (as indicated by the diameter of the clear zone) of ESN compared to RSN against *P acnes* [34,35]. However, its power to prevent the development of bacterial resistance to ESN and RSN was also observed [36].

The presence of silver atoms in the solution was observed using UV-Visible spectroscopy [37]. The size of silver atoms was determined using dynamic light scattering [38]. Efficacy and power to prevent the development of resistance were carried out using the Kirby-Bauer method [39]. The efficacy of ESN and RSN at 10 ppm and 30 ppm was compared, t-test analysis was performed and the results are discussed thoroughly in this paper. Both results were also compared with 5% Chloramphenicol [40].

2. Results

2.1. Comparison of Solution Colours

Figure 2(a) shows a photograph of four samples ESN (10 ppm and 30 ppm) and RSN (10 ppm and 30 ppm) for color comparison. Figure 2 (b) shows the increase of ESN concentration (ppm) with time (min). The difference in color is discussed later.

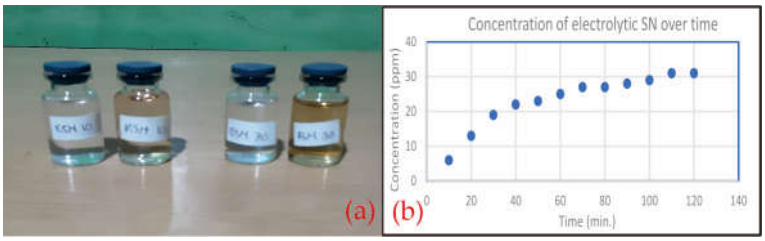

Figure 2. (a) ESN and RSN Color and (b) ESN concentration over time.

2.2. Silver Content in Solution

Figure 3 depicts the results of UV visible spectrometer measurements on the absorption peak wavelengths of ESN and RSN at 10 ppm (A) and 30 ppm (B). The possible cause of different peaks will be discussed.

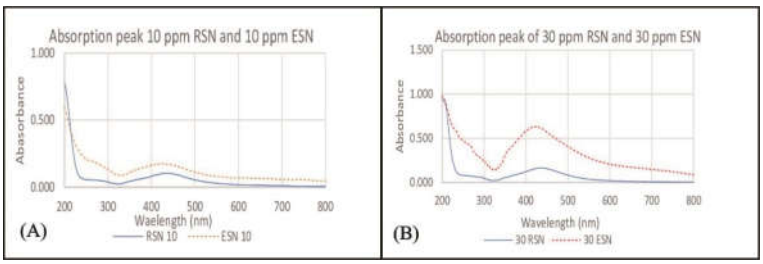

Figure 3. Absorption peaks: (A) 10ppm and (B) 30 ppm of ESN and RSN.

 doi:10.20944/preprints202412.0951.v1

2.3. Particle Size Comparison

Table 2 shows data on average particle sizes of ESN and RSN and polydispersity index (PDI) of ESN and RSN solutions. Figure 2 (b) shows the increase of ESN concentration with time during electrolysis process.

Table 1. Diameter of ESN and RSN.

Concentration (ppm)	ESN		RSN	
	Diameter (nm)	PDI	Diameter (nm)	PDI
10	40.3	0.0533	74	0.2848
30	39.9	0.0642	74.6	0.2948

2.4. Efficacy and Power to Prevent Resistance

Figure 4 (a) shows the results of clear zone diameter measurements of ESN (10 ppm), RSN (10 ppm), and Chloramphenicol (5%). Figure 4 (b) shows the results of clear zone diameter measurements of ESN (30 ppm), RSN (30 ppm), and Chloramphenicol (5%). Table 2 shows P two-tailed values of statistical analysis.

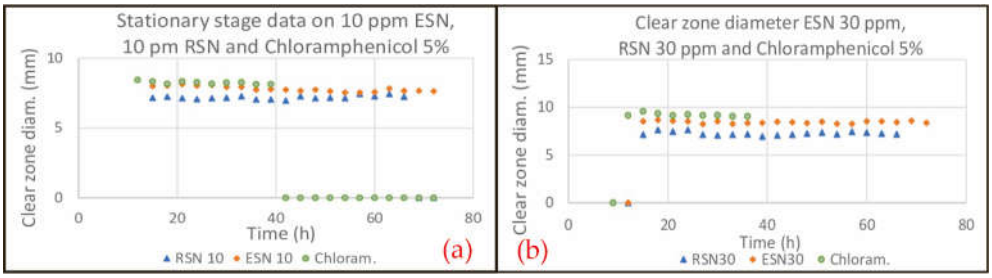

Figure 4. Clear zone diameter of (a) 10ppm and (b) 30 ppm of all antibiotics.

Table 2. P two-tail values of comparison Chloramphenicol and both types of SN.

1	Chloramphenicol (%)	ESN (ppm)	RSN (ppm)	P two-tail value
2	5	10	-	4.81×10^{-18}
3	5	30	-	3.91×10^{-8}
4	5	-	10	2.4×10^{-9}
5	5	-	30	4.61×10^{-16}
6	-	10	10	2.26×10^{-13}
7	-	30	30	7.91×10^{-20}
8	-	30:10	-	3.22×10^{-14}
9	-	-	30:10	0.254671

3. Discussions

3.2. Comparison of Solution Colours

Figure 2 (a) show the difference in color of ESN and ESN solutions. The far-left sample is 10 ppm ESN and the one next to it is RSN 10 ppm. It can be seen clearly that 10ppm ESN is much clear than 10 ppm RSN. The RSN (10 ppm) is slightly yellowish. The same color difference also occurs between 30 ppm ESN and 30 ppm RSN (far right). Here 30 ppm RSN is much yellow reddish compared to all other samples. This most likely caused by the presence of NO_2 gas which is yellowish brown and sparingly dissolves in water (see Equation 3) [41]. As for ESN the color of solution relatively remains unchanged, since there is no byproduct left nor NO_2 in the solution.

 doi:10.20944/preprints202412.0951.v1

3.2. Silver Content in Solution

UV-Visible spectrophotometer showed that the peak absorption wavelengths of 10 ppm ESN and RSN were 425 nm and 437 nm, respectively, as shown in Figure 3(A). The same peaks were shown for 30 ppm ESN and RSN in Figure 3(B). The peak wavelengths between 400-450 nm indicated the presence of silver [42]. Each graph showed only one peak which means that only silver atoms contributed to the light absorption in ESN and RSN solutions.

The data in Figure 3 show three interesting phenomena to discuss. First, both ESN concentrations show the same peak at 425 nm [43], whereas both RSN concentrations show the same peak at 437 nm [44]. This means that the dilution process does not change the content of ESN and RSN.

Second, there is a difference in the peak wavelength of absorption between ESN and RSN. This means that the peak wavelength of RSN is shifted to the right (red shift 12 nm). This is most likely related to the presence of bathochromic carboxyl in RSN solution [45], because there are three carboxyl functional groups and one hydroxyl functional group in each molecule of citric acid by-product, where carboxyl and hydroxyl are known as bathochromic auxochrome which shifts the peak to the red, to a larger wavelength. Finally, the absorbance of RSN is lower than ESN for both concentrations. This low absorbance is due to the hypochromic effect of hydroxyl functional group [46]. Some chromophores such as hydroxyl cause hypochromic effects by absorbing more light intensity. The absorption of light intensity by hydroxyl causes the absorbance to decrease. In addition, low pH is also known to cause a hypochromic effect by reducing the absorbance. RSN solution contains citric acid so that its pH is lower than ESN. Kiani et al showed the hypochromic effect of pH up to 34%[47]

3.3. Particle Size Comparison

The data presented in Table 1 show that the diameters of both types of silver nanoparticles remain relatively stable across different concentrations, indicating that adding a small amount of water to dilute the silver nanoparticles solution does not change the particle size. Table 1 also shows that RSN diameter is significantly larger than that of ESN. This may be due to the presence of reductants in the solution which helps accelerate the aggregation of silver nanoparticles. The small size of ESN can be attributed to the slow electrolysis process to form silver atoms and thus form the aggregation of ESN. As the electrolysis progresses, the formation of bubbles on the cathode increases and the cathode appears darker. The bubbles and dark layers on the cathode surface inhibit the formation of silver [48]. Figure 2 (b) shows that 22 ppm of ESN was produced during the first 40 min, but only 9 ppm was produced during the last 80 min. Meanwhile, the simultaneous redox reaction between $AgNO_3$ and $Na_3C_6H_5O_7$ resulted in the rapid production and aggregation of RSN. Therefore, the size of RSN (10 ppm and 30 ppm) was significantly larger than that of ESN (10 ppm and 30 ppm).

The PDI of RSN (0.2848 and 0.2948) was also larger than that of ESN (0.0533 and 0.0642). This indicates that the size distribution of RSN is more heterogeneous than that of ESN [49]. It is understandable that ESN is highly homogeneous because unlike RSN, no byproducts are left in the ESN solution. The average particle size and PDI data are submitted as supplementary material Data S1.

3.4. Efficacy and Power to Prevent Resistance

To explain the data analysis of antibacterial activity, we introduce three stages of antibacterial action to combat bacteria growing on a nutrient agar (NA) rich dish. The first stage is the "initial stage" [50]. This stage is relative short, begins with the placement of impregnated disks, ends with the start of stationary stage. The initial stage typically lasts only a few hours. The second stage is the "stationary stage". In this stage, the death bacteria number is approximately equals to the created bacteria number. The clear zone diameter is relatively stable and this clear zone diameter represents the efficacy of antibacterial agent. If the bacteria develop resistance to antibacterial agent, this stage

 doi:10.20944/preprints202412.0951.v1

will be relatively short, and the antibacterial agent will be rendered ineffective. Therefore, the duration time of the stationary stage represents the strength of antibacterial agent to fight against antibacterial resistance [51]. For an antibacterial agent to be considered powerful against resistance, the stationary stage should last longer, delaying the final stage. The final stage begins when the clear zone diameter consistently decreases due to resistance development which relates to stronger bacterial growth [52] until the clear zone disappears completely. By understanding these three stages, it is reasonable to compare the efficacy of different antibacterial agents during this stationary stage.

Figure 4 (a) shows the stationary stage for 10 ppm concentration of RSN, ESN, and 5% Chloramphenicol. Both RSN and ESN demonstrated antibacterial activity, as indicated by their clear zone diameters. However, ESN exhibited stronger efficacy than RSN, as evidenced by its consistently larger diameter and longer duration in preventing the spread of *P. acnes*. The statistical analysis shows that 10 ppm ESN produced significantly larger clear zone diameter than 10 ppm RSN as shown by P two-tail value=2.26×10^{-13} (see Table 2, row 6 column 5) which is smaller than 0.05 so that the null hypothesis (Ho) is rejected. The superiority of 10 ppm ESN than 10 pm RSN is probably due to its smaller size which allows it to be easier to penetrate the *P. acnes* cell wall, causing membrane leakage, destruction of internal components, and the death of the bacteria [53]. Conversely, larger sizes of RSN making it more difficult to penetrate the cell wall. Additionally, the higher purity of ESN means it comprises nearly 100% active "troops" to combat the bacteria. Whereas, the RSN solution contains citric acid and sodium hydroxide byproduct meaning it has less than 100% active components. Figure 4 (a) also shows that Chloramphenicol exhibits better efficacy than 10 ppm ESN and 10 ppm RSN, as indicated by its larger clear zone diameter. P values of the two comparisons between Chloramphenicol and 10 ppm ESN (4.81×10^{-18}), and between Chloramphenicol and 10 ppm RSN (2.4×10^{-9}) are smaller than 0.05 so that Ho is rejected meaning Chloramphenicol produces significantly larger efficacy than 10ppm ESN and 10 ppm RSN (see row 2 column 5 and row 4 column 5 of Table 2). Statistical analysis is provided in supplementary material Data S2.

However, Chloramphenicol's effectiveness lasts only 39 hours, whereas ESN and RSN remain effective for 72 hours and 66 hours, respectively. These results indicate that *P. acnes* exhibits strong resistance to Chloramphenicol, rendering this antibacterial agent is ineffective against *P. acnes* after 39 hours [54]. In contrast, *P. acnes* shows slower resistance to RSN beginning at 66 hours, and does not show resistance to ESN till the end of observation at 72 hours. This suggests that while Chloramphenicol initially has a higher efficacy, its effectiveness diminishes more rapidly due to antibacterial resistance [55]. It is well known that *P. acnes* shows resistance to many antibiotics [8,56,57]. ESN not only maintains its antibacterial activity for a longer time but also shows the power to prevent resistance development of *P. acnes*. This finding highlights the potential advantages of ESN over Chloramphenicol and RSN.

Figure 4 (b) shows the stationary stage of clear zone diameters for 30 ppm ESN, RSN, and 5% Chloramphenicol. All three antibacterial agents exhibited antibacterial activity, with Chloramphenicol being the strongest and RSN the weakest. This indicates that both ESN and RSN have potential as antibacterial agents, as their clear zone diameters were only slightly smaller than that of Chloramphenicol. A t-Test analysis shows that P values of the comparisons of Chloramphenicol 5% and 30 ppm ESN and 30 ppm RSN are 3.91×10^{-8} and 4.61×10^{-16}, respectively (see Table 2, Row 3, Column 5 and Row 5, Column 5). Both P values are smaller than 0.05 so that Ho is rejected meaning that Chloramphenicol 5% produced significantly higher efficacy than 30 ppm ESN and RSN. When comparing 30 ppm ESN and RSN, the P two-tail value of the comparison is 7.91×10^{-20} which is lower than 0.05 meaning that 30 ppm ESN produced significantly higher efficacy than 30 ppm RSN.

Figure 4 (b) also shows that the stationary stage of Chloramphenicol ceased at 36 h, RSN stopped at 66 h, and ESN ceased at 72 h (the last observation). These facts show that 5% Chloramphenicol is the weakest in preventing *P. acnes* resistance development, ESN is the strongest (having twice power than Chloramphenicol), and RSN is weaker than ESN. The ability of ESN to maintain its efficacy without inducing antibacterial resistance highlights its potential superiority over RSN and Chloramphenicol.

 doi:10.20944/preprints202412.0951.v1

P values of statistical analysis of the comparison between 30 ppm and 10 ppm RSN is 0.254671 (Table 2, row 9 column 5) which is higher than 0.05. Therefore, Ho is accepted meaning that 30 ppm RSN does not produce significantly larger efficacy than 10 ppm RSN. On the contrary, 30 ppm ESN produced significantly higher efficacy than 10 ppm ESN as indicated by P value of 3.22×10^{-14} which is less than 0.05 (see Table 2, Row 8, Column 5). This means that higher ESN concentration produces higher efficacy. This trend can be used to estimate the efficacy of ESN at higher concentration. However, our data are limited to 10 ppm and 30 ppm ESN, so that they are not sufficient to draw a reliable calibration curve. Assuming two data points are sufficient to draw a calibration curve, this results in a linier regression equation of Y=0.0314X + 7.4936. By using this equation ESN of 54.34 ppm would results in a clear zone diameter equivalent to that of 5% Chloramphenicol which is 9.2 mm. It should be noted that this ESN concentration is very low, since 54.34 ppm approximately equals to 0.005% which is much lower than that of 5% Chloramphenicol. The superiority of ESN over Chloramphenicol is probably due to bactericidal property of ESN compared to bacteriostatic of Chloramphenicol. ESN kills and inhibits bacteria in many different mechanisms as depicted in Figure 7. These findings show convincingly the superiority of ESN as antibacterial agent over Chloramphenicol which underscores compelling potential as raw material for future antibacterial agent.

4. Material and Method

4.1. RSN Production

The precursor 100 ml of 10 mM silver nitrate (AgNO3) was prepared by dispersing 170 mg of $AgNO_3$ powder with water to a total volume of 100 ml. The mixture was homogenized by stirring on magnetic stirrer at 50 rpm 25oC for 5 minutes. The 100 ml of 10 mM stabilizer was prepared by mixing 258mg $Na_3C_6H_5O_7$ with water up to 100 ml. No specific reducing agent was introduced, since trisodium citrate is also reducing agent [58]. The balance reaction is given by

$$12AgNO_3 + 4Na_3C_6H_5O_7 + 6H_2O \leftrightarrow 12\text{Ag} + 12\text{NaN}O_3 + 4C_6H_8O_7 + 3O_2. \quad (1)$$

Based on Equation (2) in a single reaction, this technique produces 12 silver atoms, 12 $NaNO_3$, 4 $C_6H_8O_7$, and 3 oxygen gas. All of them remains in the solution except oxygen gas. Citric acid with chemical formula HOC(CO2H)(CH2CO2H)2 contains three carboxyl (CO2H) and hydroxyl (OH) functional groups [59]. Citric acid is soluble in water and considered to be contaminant in RSN solution since there no easy method to separate citric acid from water as solvent of the RSN solution.

Another major by product NaNO3 is soluble in water and it dissociate in water to form Na^+ and $NO3^-$. This $NO3^-$ in water react quickly with H^+ ion to form HNO_3 which then decomposes to form NO_2, H_2O, and O_2. Here is the complete reaction:

$$\mathbf{4NaNO_3 \leftrightarrow 4Na^+ + 4NO_3^-}$$
$$\mathbf{4H_2O \leftrightarrow 4H^+ + 4OH^-}$$
$$\mathbf{4Na^+ + 4OH^- \leftrightarrow 4NaOH}$$
$$\mathbf{4H^+ + 4NO_3^- \leftrightarrow 4HNO_3}$$
$$\mathbf{4HNO_3 \leftrightarrow 4NO_2 + 2H_2O + O_2}$$
$$\mathbf{4NaNO_3 + 2H_2O \leftrightarrow 4NO_2 + 4NaOH + O_2}. \quad (2)$$

NO_2 by product on the right-hand side of Equation 3 is yellowish brown toxic gas which is sparingly dissolved in water to give yellowish colour of the RSN solution. Another byproduct of this reduction technique is NaOH as shown on the right had side of Equation 3. Therefore, there are two contaminants present in RSN solution which are $C_6H_8O_7$ and NaOH. The process of RSN formation is depicted in Figure 5 (a) mixing and heating precursor and reductor, (b) silver atoms production, and (c) silver nanoparticle aggregation and toxic gas byproduct.

Preprints.org (www.preprints.org) | NOT PEER-REVIEWED | Posted: 12 December 2024 doi:10.20944/preprints202412.0951.v1

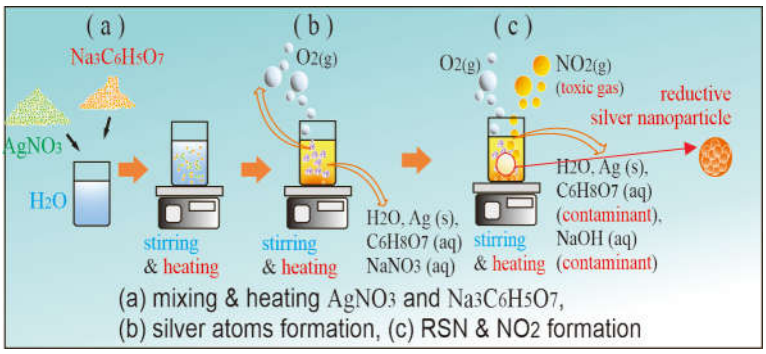

Figure 5. Reductive silver nanoparticles formation.

The stock sample was prepared by adding 2 ml of 10mM precursor and 2 ml of 10mM stabilizer to a conical flask containing 36 ml of water. The concentration of silver was diluted by a factor of 1/20to become 1079 ppm/20, which equals 54 ppm. This 54-ppm RSN is marked as stock solution. The 30 ppm and 10 ppm RSN concentrations were diluted from this stock solution.

4.2. ESN Production

An electrolysis unit consisting of a 500 ml capacity of brown bottle, two identical silver plates electrodes, black rubber bottle lid, 24-volt DC power supply, 400 ml of distilled water, and two pieces of electrical cable was used to produce ESN solution. The dimension of each silver plate is 16 cm in length, 4 cm in width, and 0.2 cm in thickness. The DC power supply is set at 24 V and 5 A.

Modifications were made to two parts of the electrolysis system. First, replacing silver nitrate as the electrolyte with water. This was done because the source of the toxic gas NO2 was silver nitrate. However, by replacing silver nitrate as the electrolyte at the same time, the source of silver atoms was also lost. This led to the second modification, which was replacing the electrodes (which are usually a silver rod and a carbon rod) with two identical silver plates. Since two identical silver plates are used as electrodes, the electrical wiring connections can be made with any choice. The anode and cathode are interchangeable. Plates were chosen instead of rods to increase the surface area of the electrodes facing each other to increase the production of silver atoms. The replacement of silver nitrate solution as electrolyte with water was taken after careful consideration that the replacement of silver nitrate with silver chloride, silver bromide, or silver iodide also produces chlorine gas (Cl_2), bromine gas (Br_2) or iodine gas (I_2) and all of them are toxic.

Ag+ ions released from the anode go to the cathode, some of which capture electrons in the solution to form silver atoms that remain in the solution to form ESN [13] and some of which are neutralized by electrons on the cathode to coat the cathode surface. The equilibrium reaction of the production of ESN is given by

$$2Ag^{+}(aq) + 2H_2O \leftrightarrow 2\text{Ag (aq)} + H_2(g) + 2H^{+} + O_2(g). \quad (3)$$

The products on the right-hand side of Equation 3 are all gases except the silver atoms. H2 and O2 are friendly gases and return to nature. 2H+ turns into H2 gas as soon as it encounters electrons to form a covalent bond between the two H atoms. There is no contaminant, nor toxic gases produced in this modified electrolysis. Figure 6 depicts ESN formation involving (1) oxidation producing silver ions in anode, (2) reduction in solution and in cathode resulting in silver atoms, (3) silver atoms aggregation, and (4) ESN formation.

Preprints.org (www.preprints.org) | NOT PEER-REVIEWED | Posted: 12 December 2024 doi:10.20944/preprints202412.0951.v1

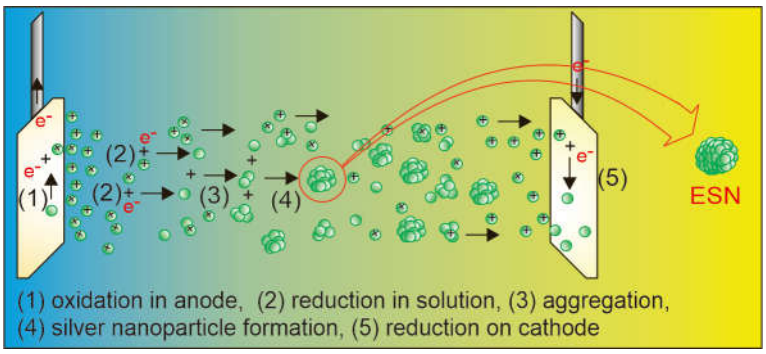

Figure 6. Electrolytic silver nanoparticles formation.

A stock of 400 ml of 31 ppm is produced within 2 h as shown in Figure 2 (b). This stock sample was diluted to 30 ppm and 10 ppm using this simple equation $\boldsymbol{C_1V_1 = C_2V_2}$ where C_1 is 31 ppm stock solution, V_1 is the calculated stock volume in ml, C_2 is target concentration (30 ppm or 10 ppm), and V_2 is 100 ml target volume. The volume $V_1=(V_2C_2)/C_1$= (100 ml x 30 ppm)/31 ppm = 96.77 ml. Therefore, 100 ml volume of 30 ppm sample of ESN was made by adding 96.77 ml stock with 3.23 ml water. A 100 ml of 10 ppm ESN was prepared in the same way.

4.3. Observation of Solution Colour

Observation of solution colors was done by taking photograph of 10 ppm and 30 ppm ESN and 10 ppm and 30 ppm RSN. All of them were taken in a single frame. Photograph was taken using a tablet Samsung S6 and converted into .jpg and finally its resolution (dpi) was increased to 600 dpi.

4.4. Detection of Silver in Solution

The presence of silver atoms in the solution was detected using UV visible spectrophotometer. The solution was scanned from 200nm to 800 nm to find the absorption peak wavelength. The measurement is presented in form of a graph of absorbance as a function of wavelength of light. The presence of silver atoms or any other atoms will be identified by its peak wavelength. If 3 different types of atoms presence in the same solution the graph will show 3 absorption peaks.

4.5. Particle Size Determination

The determination of particle size was conducted using the Laser Amplified Detection (LAD) method, a cutting-edge advancement of the Dynamic Light scattering (DLS) technique [38]. Unlike UV visible spectrophotometer and other traditional light scattering system requiring 4 ml of sample, LAD requires only 5 microliter volume of sample. Since the sample is very small, a precise sample preparation is needed. The presence of contaminant and aggregate in such a small size of sample would destroy the measurement. In case this happens, the measurement must be repeated using a new sample taken from the same stock. The result of the measurement is presented in form of size distribution graph (gaussian like graph) with one peak and the value of polydispersity index. The polydispersity index shows the homogeneity of the solution and the peak of Gaussian graph shows the mean diameter of particles dispersed in the solution.

4.6. Antibacterial Activity Observation

Preparation of nutrient broth and nutrient agar was done in the same way as previous publication [11]. Bacteria used in this research was *Propionibacterium acnes* ATCC 6919 strain NCTC 737 (VPI 0389). The antibacterial activity of ESN (10 ppm and 30) ppm), ESN (10 ppm and 30 ppm), and Chloramphenicol 5% (positive control) was assessed in a petri dish containing NA and *P. acnes*. Clear zone diameter was measured once in 3 hours at 3 different positions (horizontal, vertical, and diagonal) for a period of 72 h.

 doi:10.20944/preprints202412.0951.v1

5. Conclusion

In summary, physical characteristics of ESN is better than RSN. ESN colour is clear like water whereas RSN is yellowish due to dissolves yellowish toxic gas NO_2. Unlike RSN, there is no NO_2 in ESN solution. ESN absorption peak wavelength is lower meaning there is no bathochromic auxochrome in the ESN solution. ESN size is much smaller meaning that it is easier to penetrate bacteria cell wall. ESN PDI is also much lower showing that ESN is much more homogeneous than RSN.

As for antibacterial efficacy ESN shows higher efficacy than RSN. Unlike RSN, efficacy of ESN increases with the increase of concentration. Based on this trend, a calibration curve maybe drawn with linier regression equation which can be used to predict efficacy of higher ESN concentration. Based on the linier regression equation, it was found that 9.2 nm clear zone diameter produced by 5% Chloramphenicol can be produced by 54.34 ppm ESN which is approximately equal to 0.005%. This ESN concentration is still much lower than 5% Chloramphenicol. This means that the efficacy of ESN is not only superior compared to RSN but also to Chloramphenicol. This finding underscores the potential of ESN as raw material for future antibiotics.

Although Chloramphenicol initially exhibits the highest efficacy, its effectiveness is short-lived (after 36 h) due to rapid development of *P. acnes* resistance. Despite showing strong resistance to 5% Chloramphenicol, *P. acnes* also shows weak resistance to RSN. In contrast, *P. acnes* does not show any resistance development to ESN up to the last measurement at 72 h. The prolonged efficacy and the strength to prevent bacterial resistance development make ESN a promising alternative for future antibiotics raw material, potentially offering more durable and effective solutions for combating microbial infections.

Supplementary Material: The following supporting information can be downloaded at the website of this paper posted on Preprints.org.

References

1. Breijyeh Z and Karaman R 2023 Design and Synthesis of Novel Antimicrobial Agents *Antibiotics* **12**
2. Lei J, Sun L C, Huang S, Zhu C, Li P, He J, Mackey V, Coy D H and He Q Y 2019 The antimicrobial peptides and their potential clinical applications *Am J Transl Res* **11**
3. Patangia D V., Anthony Ryan C, Dempsey E, Paul Ross R and Stanton C 2022 Impact of antibiotics on the human microbiome and consequences for host health *Microbiologyopen* **11**
4. Fair R J and Tor Y 2014 The Rise of Antibiotic Resistance *Perspect Medicin Chem* **6**
5. Reding C, Catalán P, Jansen G, Bergmiller T, Wood E, Rosenstiel P, Schulenburg H, Gudelj I and Beardmore R 2021 The Antibiotic Dosage of Fastest Resistance Evolution: Gene Amplifications Underpinning the Inverted-U *Mol Biol Evol* **38**
6. Muteeb G 2023 Nanotechnology—A Light of Hope for Combating Antibiotic Resistance *Microorganisms* **11**
7. Pila G, Segarra D and Cerna M 2023 Antibacterial effect of Cannabidiol oil against Propionibacterium acnes, Staphylococcus aureus, Staphylococcus epidermidis and level of toxicity against Artemia salina *Bionatura* **8**
8. Achermann Y, Goldstein E J C, Coenye T and Shirtliffa M E 2014 Propionibacterium acnes: From Commensal to opportunistic biofilm-associated implant pathogen *Clin Microbiol Rev* **27**
9. Bronnec V, Eilers H, Jahns A C, Omer H and Alexeyev O A 2022 Propionibacterium (Cutibacterium) granulosum Extracellular DNase BmdE Targeting Propionibacterium (Cutibacterium) acnes Biofilm Matrix, a Novel Inter-Species Competition Mechanism *Front Cell Infect Microbiol* **11**
10. Bourguignon N, Kamat V A, Lerner B, Perez M and Bhansali S 2019 The Use of Lab on a Chip Devices to Evaluate Infectious Biofilm Formation and Assess Antibiotics and Nano Drugs Treatments *ECS Meeting Abstracts* **MA2019-01**
11. Suparno S, Ayu Lestari E S and Grace D 2024 Antibacterial activity of Bajakah Kalalawit phenolic against Staphylococcus aureus and possible use of phenolic nanoparticles *Sci Rep* **14** 19734
12. Tan Z, Deng J, Ye Q and Zhang Z 2022 The Antibacterial Activity of Natural-derived Flavonoids *Curr Top Med Chem* **22**
13. Girma A 2023 Alternative mechanisms of action of metallic nanoparticles to mitigate the global spread of antibiotic-resistant bacteria *The Cell Surface* **10**

 doi:10.20944/preprints202412.0951.v1

14. Singh I, Mazhar T, Shrivastava V and Singh Tomar R 2022 Bio-assisted synthesis of bi-metallic (Ag-Zn) nanoparticles by leaf extract of Azadirachta indica and its antimicrobial properties *International Journal of Nano Dimension* **13**
15. Prasad S R, Teli S B, Ghosh J, Prasad N R, Shaikh V S, Nazeruddin G M, Al-Sehemi A G, Patel I and Shaikh Y I 2021 A Review on Bio-inspired Synthesis of Silver Nanoparticles: Their Antimicrobial Efficacy and Toxicity *Engineered Science* **16**
16. Liao C, Li Y and Tjong S C 2019 Bactericidal and cytotoxic properties of silver nanoparticles *Int J Mol Sci* **20**
17. Pletikapić G, Žutić V, Vinković Vrček I and Svetličić V 2012 Atomic force microscopy characterization of silver nanoparticles interactions with marine diatom cells and extracellular polymeric substance *Journal of Molecular Recognition* vol 25
18. Veeraraghavan V P, Periadurai N D, Karunakaran T, Hussain S, Surapaneni K M and Jiao X 2021 Green synthesis of silver nanoparticles from aqueous extract of Scutellaria barbata and coating on the cotton fabric for antimicrobial applications and wound healing activity in fibroblast cells (L929) *Saudi J Biol Sci* **28**
19. Lethongkam S, Paosen S, Bilhman S, Dumjun K, Wunnoo S, Choojit S, Siri R, Daengngam C, Voravuthikunchai S P and Bejrananda T 2022 Eucalyptus-Mediated Synthesized Silver Nanoparticles-Coated Urinary Catheter Inhibits Microbial Migration and Biofilm Formation *Nanomaterials* **12**
20. Durán N, Durán M, de Jesus M B, Seabra A B, Fávaro W J and Nakazato G 2016 Silver nanoparticles: A new view on mechanistic aspects on antimicrobial activity *Nanomedicine* **12**
21. Hume S L, Chiaramonti A N, Rice K P, Schwindt R K, MacCuspie R I and Jeerage K M 2015 Timescale of silver nanoparticle transformation in neural cell cultures impacts measured cell response *Journal of Nanoparticle Research* **17**
22. Gordon O, Slenters T V, Brunetto P S, Villaruz A E, Sturdevant D E, Otto M, Landmann R and Fromm K M 2010 Silver coordination polymers for prevention of implant infection: Thiol interaction, impact on respiratory chain enzymes, and hydroxyl radical induction *Antimicrob Agents Chemother* **54**
23. Thammawithan S, Talodthaisong C, Srichaiyapol O, Patramanon R, Hutchison J A and Kulchat S 2022 Andrographolide stabilized-silver nanoparticles overcome ceftazidime-resistant Burkholderia pseudomallei: study of antimicrobial activity and mode of action *Sci Rep* **12**
24. Li A, Zheng N and Ding X 2022 Mitochondrial abnormalities: a hub in metabolic syndrome-related cardiac dysfunction caused by oxidative stress *Heart Fail Rev* **27**
25. Raisanen A L, Mueller C M, Chaudhuri S, Schatz G C and Kushner M J 2022 A reaction mechanism for plasma electrolysis of AgNO3forming silver nanoclusters and nanoparticles *J Appl Phys* **132**
26. Naderi-Samani E, Razavi R S, Nekouee K and Naderi-Samani H 2023 Synthesis of silver nanoparticles for use in conductive inks by chemical reduction method *Heliyon* **9**
27. Yantcheva N S, Karashanova D B, Georgieva B C, Vasileva I N, Stoyanova A S, Denev P N, Dinkova R H, Ognyanov M H and Slavov A M 2019 Characterization and application of spent brewer's yeast for silver nanoparticles synthesis *Bulgarian Chemical Communications* **51**
28. Wahab S, Khan T, Adil M and Khan A 2021 Mechanistic aspects of plant-based silver nanoparticles against multi-drug resistant bacteria *Heliyon* **7**
29. Roy A, Bulut O, Some S, Mandal A K and Yilmaz M D 2019 Green synthesis of silver nanoparticles: Biomolecule-nanoparticle organizations targeting antimicrobial activity *RSC Adv* **9**
30. Sadiq M U, Shah A, Haleem A, Shah S M and Shah I 2023 Eucalyptus globulus Mediated Green Synthesis of Environmentally Benign Metal Based Nanostructures: A Review *Nanomaterials* **13**
31. Ezealisiji K M, Noundou X S and Ukwueze S E 2017 Green synthesis and characterization of monodispersed silver nanoparticles using root bark aqueous extract of annona muricata linn and their antimicrobial activity *Applied Nanoscience (Switzerland)* **7**
32. J. Kasprowicz M, Gorczyca A and Janas P 2016 Production of Silver Nanoparticles Using High Voltage Arc Discharge Method *Curr Nanosci* **12**
33. Hidayah A N, Triyono D, Saputra A B, Herbani Y, Isnaeni I and Suliyanti M M 2019 Stabilization of Au-Ag Nanoalloys with Polyvinylpyrrolidone (PVP) as Capping Agent *Journal of Physics: Conference Series* vol 1191
34. Amer S S, Mamdouh W, Nasr M, ElShaer A, Polycarpou E, Abdel-Aziz R T A and Sammour O A 2022 Quercetin loaded cosm-nutraceutical electrospun composite nanofibers for acne alleviation: Preparation, characterization and experimental clinical appraisal *Int J Pharm* **612**
35. Mohd Danial A, Koh S P, Abdullah R and Azali A 2020 Evidence of potent antibacterial effect of fermented papaya leaf against opportunistic skin pathogenic microbes *Food Res* **4**
36. de Mello M S and Oliveira A C 2021 Challenges for adherence to bacterial resistance actions in large hospitals *Rev Bras Enferm* **74**
37. Kaidi S, Belattmania Z, Bentiss F, Jama C, Reani A and Sabour B 2022 Synthesis and characterization of silver nanoparticles using alginate from the brown seaweed laminaria ochroleuca: Structural features and antibacterial activity *Biointerface Res Appl Chem* **12**

38. Jia Z, Li J, Gao L, Yang D and Kanaev A 2023 Dynamic Light Scattering: A Powerful Tool for In Situ Nanoparticle Sizing *Colloids and Interfaces* **7**
39. Alhamadani Y and Oudah A 2022 Study of the Bacterial Sensitivity to different Antibiotics which are isolated from patients with UTI using Kirby-Bauer Method *Journal of Biomedicine and Biochemistry*
40. Singhal K K, Mukim M, Dubey C K and Nagar J C 2020 An Updated Review on Pharmacology and Toxicities Related to Chloramphenicol *Asian Journal of Pharmaceutical Research and Development* **8**
41. Huffman C F 1959 Dairy Feeds and Drug Additives as Related to Cattle Efficiency and Public Health *J Dairy Sci* **42**
42. Najafi A, Khoeini M, Khalaj G and Sahebgharan A 2021 Synthesis of silver nanoparticles from electronic scrap by chemical reduction *Mater Res Express* **8**
43. Zanjage A and Khan S A 2021 Ultra-fast synthesis of antibacterial and photo catalyst silver nanoparticles using neem leaves *JCIS Open* **3**
44. Subramanyam G K, Gaddam S A, Kotakadi V S, Gunti H, Palithya S, Penchalaneni J and Challagundla V N 2023 Green Fabrication of silver nanoparticles by leaf extract of Byttneria Herbacea Roxb and their promising therapeutic applications and its interesting insightful observations in oral cancer *Artif Cells Nanomed Biotechnol* **51**
45. Chernii S, Selin R, Tretyakova I, Dovbiy Y, Pekhnyo V, Rotaru A, Chernii V, Kovalska V and Mokhir A 2023 Synthesis and photophysical properties of indolenine styrylcyanine dye and its carboxyl-labeled derivative *Biointerface Res Appl Chem* **13**
46. Rasheed Z, Alharbi A, Alrakebeh A, Almansour K, Almadi A, Almuzaini A, Salem M, Aloboody B, Alkobair A, Albegami A, Alhomaidan H T, Rasheed N, Alqossayir F M, Musa K H, Hamad E M and Al Abdulmonem W 2022 Thymoquinone provides structural protection of human hemoglobin against oxidative damage: Biochemical studies *Biochimie* **192**
47. Kiani Nejad Z, Mirzaei-Kalar Z and Khandar A A 2021 Synthesis of ZnFe2O4@SiO2 nanoparticles as a pH-sensitive drug release system and good nano carrier for CT-DNA binding *J Mol Liq* **339**
48. Seweryn J, Biesdorf J, Boillat P and Schmidt T J 2015 Neutron Radiography of PEM Water Electrolysis Cells *ECS Meeting Abstracts* **MA2015-03**
49. Manconi M, Manca M L, Caddeo C, Cencetti C, di Meo C, Zoratto N, Nacher A, Fadda A M and Matricardi P 2018 Preparation of gellan-cholesterol nanohydrogels embedding baicalin and evaluation of their wound healing activity *European Journal of Pharmaceutics and Biopharmaceutics* **127**
50. Sacher E 2022 A Pragmatic Perspective of the Initial Stages of the Contact Killing of Bacteria on Copper-Containing Surfaces *Appl Microbiol* **2**
51. Xiao L, Hui F, Tian T, Yan R, Xin J, Zhao X, Jiang Y, Zhang Z, Kuang Y, Li N, Zhao Y and Lin Q 2021 A Novel Conductive Antibacterial Nanocomposite Hydrogel Dressing for Healing of Severely Infected Wounds *Front Chem* **9**
52. Ning Q, Wang D, An J, Ding Q, Huang Z, Zou Y, Wu F and You J 2022 Combined effects of nanosized polystyrene and erythromycin on bacterial growth and resistance mutations in Escherichia coli *J Hazard Mater* **422**
53. Dong Y, Zhu H, Shen Y, Zhang W and Zhang L 2019 Antibacterial activity of silver nanoparticles of different particle size against Vibrio Natriegens *PLoS One* **14**
54. Arip M, Selvaraja M, Mogana R, Tan L F, Leong M Y, Tan P L, Yap V L, Chinnapan S, Tat N C, Abdullah M, Dharmendra K and Jubair N 2022 Review on Plant-Based Management in Combating Antimicrobial Resistance - Mechanistic Perspective *Front Pharmacol* **13**
55. Mu R, Zhang H, Zhang Z, Li X, Ji J, Wang X, Gu Y and Qin X 2023 Trans-cinnamaldehyde loaded chitosan based nanocapsules display antibacterial and antibiofilm effects against cavity-causing Streptococcus mutans *J Oral Microbiol* **15**
56. Dreno B, Foulc P, Reynaud A, Moyse D, Habert H and Richet H 2005 Effect of zinc gluconate on propionibacterium acnes resistance to erythromycin in patients with inflammatory acne: In vitro and in vivo study *European Journal of Dermatology* **15**
57. Nakase K, Nakaminami H, Takenaka Y, Hayashi N, Kawashima M and Noguchi N 2017 Propionibacterium acnes is developing gradual increase in resistance to oral tetracyclines *J Med Microbiol* **66**

 doi:10.20944/preprints202412.0951.v1

58. Pico P, Nathanael K, Lavino A D, Kovalchuk N M, Simmons M J H and Matar O K 2023 Silver nanoparticles synthesis in microfluidic and well-mixed reactors: A combined experimental and PBM-CFD study *Chemical Engineering Journal* **474**
59. Zabiszak M, Nowak M, Taras-Goslinska K, Kaczmarek M T, Hnatejko Z and Jastrzab R 2018 Carboxyl groups of citric acid in the process of complex formation with bivalent and trivalent metal ions in biological systems *J Inorg Biochem* **182**